# Micromechanical Membrane Switches on Silicon

A new class of electronic devices, micromechanical membrane switches, has been developed. These switches have operating characteristics that fill the gap between conventional silicon transistors and mechanical electromagnetic relays. Although they are batch fabricated on silicon using conventional photolithographic and integrated circuit processing techniques, their unique properties allow them to perform functions not ordinarily associated with silicon. The devices are basically extremely small, electrostatically controlled mechanical relays, typically less than 100  $\mu$ m long. Their high off- to on-state impedance ratio and all-metal conduction paths make them ideally suited for ac signal switching arrays. This paper describes the design, fabrication, operating behavior, and potential applications of these voltage-controlled, micromechanical switches.

## Introduction

During the last two decades silicon has proven itself to be the unsurpassed, irreplaceable electronic material. The economic and social importance of silicon integrated circuit technology is epitomized by its description [1] as "the new steel." In addition to its obvious electronic virtues, however, recent research programs have indicated that silicon also possesses unique and useful mechanical characteristics, and is now revolutionizing the way we think about precision, miniature mechanical devices and components. Ink jet nozzles [2] and charge plates [3] made from silicon-possibly with driving electronics on the same chip [4]—are under development; a complete, functioning gas chromatograph on a wafer including three-meter capillary column, sensor, and pneumatic valves has been demonstrated [5]; a miniature biomedical accelerometer with high sensitivity has been fabricated entirely from silicon [6]; silicon has been used as a high precision optical bench for positioning minute fiber-optic components and lasers [7-13]; and a series of interconnecting grooves etched in silicon are being designed to function as a microminiature Joule-Thomson cryogenic refrigerator [14]. This partial list gives some idea of the versatility and far-reaching implications of the new silicon micromechanics technology.

One aspect of silicon micromechanics we have decided to exploit is electrostatically deflectable devices fabricated from thin SiO, membranes [15, 16]: in particular, micromechanical electrical switches and optical modulating elements. Early work in this field was performed by Thomas et al. [17], who demonstrated that large, two-dimensional arrays of SiO, membranes could be fabricated and employed in electron-beam-addressed optical imaging and storage displays. Although these arrays of SiO<sub>3</sub>membrane optical modulators performed much the same function as previous metal-film deformographic [18-20] displays, they revealed the crucial advantages of thermally grown, amorphous, insulating membranes over plated or evaporated metal membranes [21, 22]. Fatigue effects and the attendant deterioration of deflection parameters are greatly reduced in thermally grown SiO, membranes. In addition, as we shall see, a significant versatility in device design is acquired. The devices described herein, for example, would not be possible without an insulating membrane material.

This paper will describe the fabrication and operation of several micromechanical membrane devices. The sections following this introduction will discuss the fundamentals of fabrication and operation; will describe the basic switch, its operating characteristics, and several possible geometries; and will examine a number of applications including a cross-point switching array for handling ac signals, circuits and arrays being investigated as

Copyright 1979 by International Business Machines Corporation. Copying is permitted without payment of royalty provided that (1) each reproduction is done without alteration and (2) the *Journal* reference and IBM copyright notice are included on the first page. The title and abstract may be used without further permission in computer-based and other information-service systems. Permission to *republish* other excerpts should be obtained from the Editor.

optical data storage cells, and a temperature sensor. The construction of micromechanical switches on arbitrary substrates will be briefly reviewed in the section following these, and finally, an outline of practical considerations and future research directions will be presented.

## **Fabrication fundamentals**

The device structures discussed here are cantilever beams composed of thin  $(0.35-\mu m)$ , metal-coated insulating membranes attached to the silicon substrate at one end and suspended over a shallow rectangular pit. This pit is produced by etching the silicon out from under the deposited insulating film in a carefully yet easily controlled etching procedure. The silicon etchant (EDP) used in this work is a hot  $(118^{\circ}C)$  solution of ethylene diamine, pyrocatechol, and water first described by Finne and Klein [23]. The following unique features make this etchant indispensable for these applications:

- 1. It has a very low etch rate for  $SiO_2$  (~10 nm/h) compared to silicon (~50  $\mu$ m/h).
- EDP does not appreciably attack chromium or gold, so that device metallizations can be patterned prior to the silicon etching.
- 3. The etch rate of silicon highly doped with boron is reduced by at least a factor of 50 [24], so that a buried p<sup>+</sup> region can be used as a vertical etch stop [15].
- 4. EDP is an anisotropic etchant whose properties make it possible to undercut the membrane regions and to define the cantilever beams without etching the silicon elsewhere. Descriptions of this undercut mechanism have been given previously [3, 16, 25] in terms of the geometry and orientation of the mask.

While the anisotropic etching behavior of EDP permits control over the extent and direction of lateral etching, a p<sup>+</sup> buried region is used to stop the etch vertically, effectively resulting in a completely self-limiting etching step. With these considerations, the fabrication of electrostatically deflectable micromechanical switches of the general form shown in Fig. 1 can be formulated. Since it is important to have a shallow well beneath the membranes for large electrostatic forces, the wafer is highly doped with boron (the *vertical* etch stop); and an epitaxial layer is grown over this doped region to a thickness d, which will correspond to the depth of the pit. SiO, is then grown to a thickness t, over which a thin Cr-Au metallization is also deposited. The metal is patterned into lines and the insulator is etched out from around the lines, defining the shape of the membrane which is shown in cross section in Fig. 2(a). After the SiO<sub>2</sub> etch, which exposes the silicon (to be etched later by EDP), photoresist layers are applied and patterned as shown in Fig. 2(b) to provide windows through which gold will be plated, and to define the mesas

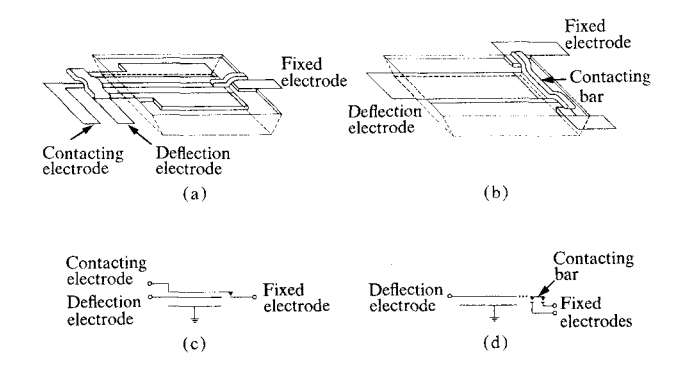


Figure 1 Two designs of micromechanical switches: (a) the single-contact low current design, and (b) the double-contact configuration; (c) and (d) are suggested circuit representations of these devices.

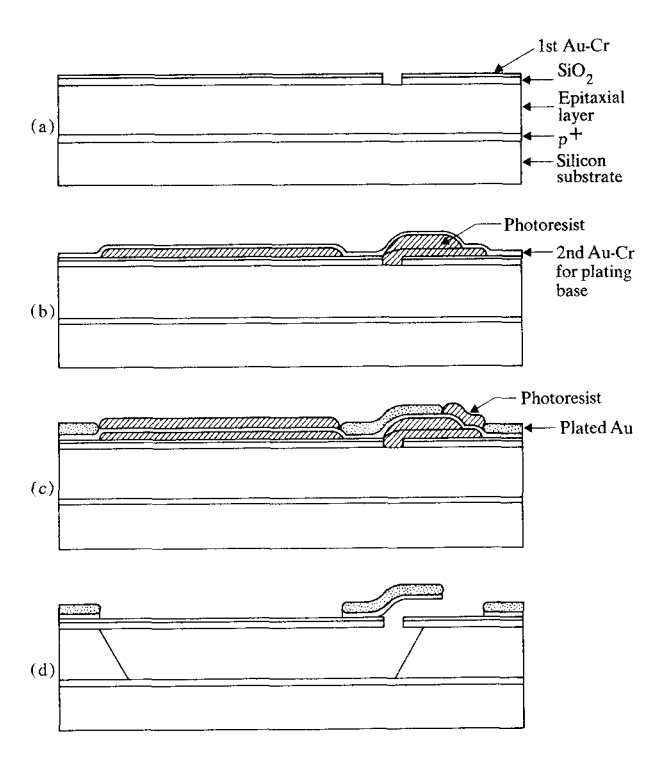


Figure 2 Cross-sectional diagrams of a single-contact micromechanical switch at various stages during the fabrication procedure: (a) after first metal etch and oxide etch; (b) after evaporation of Au-Cr plating base; (c) after Au plating through photoresist holes; (d) finished structure after photoresist removal, plating base etch, and EDP etch.

over which gold will be plated to form the bridge structures and contact-electrode projections. A second Cr-Au layer (0.3  $\mu$ m) is deposited over the wafer to serve as a plating base, and the device cross section then appears as shown in Fig. 2(b). Another photoresist application is

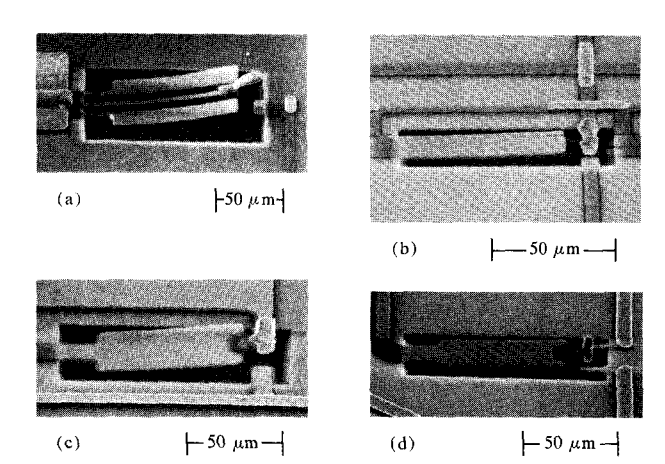


Figure 3 Four different micromechanical switch designs: (a) single-contact; (b) double-contact with a contact bar as shown in Fig. 4(c); (c) and (d) are double-contact designs with two orientations of the fixed electrodes. Note: The SEM photographs for Figs. 3, 5-7, 9, 10, and 14 were taken at an angle of approximately 65° from normal.

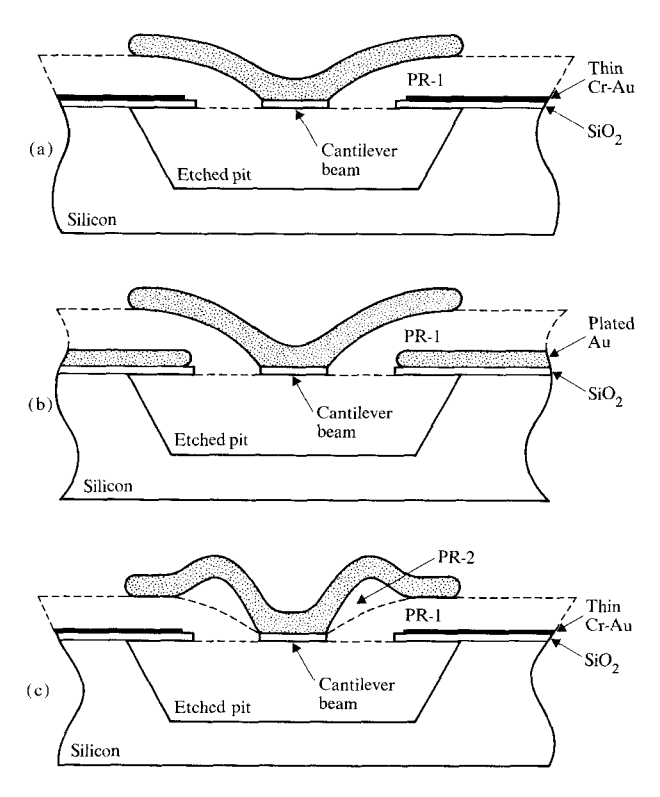


Figure 4 Contacting bar design procedure: (a) cross section of initial design exhibiting irreproducible contacting behavior. Design improvements to correct this contact problem are shown in (b) plated metal over the fixed electrodes and (c) double photoresist (PR) process.

used to define the regions to be plated, and about 2  $\mu$ m of gold is electroplated through the photoresist windows, as indicated in Fig. 2(c). Finally the photoresist layers and

excess plating base are stripped and the silicon is etched in the EDP solution for about 20 minutes, rinsed, and carefully dried. A cross section of the completed device is shown in Fig. 2(d). Scanning electron microscope (SEM) photographs of several device configurations are shown in Fig. 3.

Typical device dimensions are  $0.35 - \mu$ m-thick SiO<sub>2</sub>, 40 nm of the first Cr-Au layer, and 75- $\mu$ m-long cantilever beams, suspended over a 5- to 7- $\mu$ m-deep pit—the approximate thickness of the epitaxial layer. When a voltage is applied between the p<sup>+</sup> silicon in the bottom of the pit and the deflection electrode metallization on the membrane surface, the cantilever beam will experience an electrostatic force distributed along its length, which pulls it downward until the plated metal projection at the membrane tip makes electrical contact with the fixed electrode.

In addition to the unique design and operational characteristics to be discussed subsequently, micromechanical membrane switches exhibit noteworthy fabrication advantages. The detailed electronic quality of the silicon is not particularly critical and the device characteristics are relatively insensitive to oxide pinholes, compared to conventional silicon electronic devices.

#### Operational characteristics

These micromechanical devices are nearly ideal electrical switches, and are potentially applicable in circuits which require:

- 1. Extremely high off-state to on-state impedance ratios;
- 2. Low off-state coupling capacitance;
- 3. High device density;
- 4. Very low switching and sustaining power;
- 5. Low resistance metal-to-metal contacts;
- 6. Medium current-carrying capability; and/or
- 7. Four-terminal, fully isolated input/output lines.

Additional important advantages of micromechanical switches are the versatility available in design and fabrication and the simple, inexpensive processing (five mask levels) with minimal high-temperature cycling. Several different designs are shown in Fig. 3.

The single-contact configuration was the first successful demonstration of micromechanical switches, but it suffers from the problem that one of the current-carrying output metallizations traverses the entire length of the deflectable membrane. Since such metallizations must be thin ( $\sim 50$  nm), the current-carrying capability of the single-contact design is poor.

This problem is alleviated by the double-contact design illustrated in Figs. 1(b), 3(b), 3(c), and 3(d), in which the

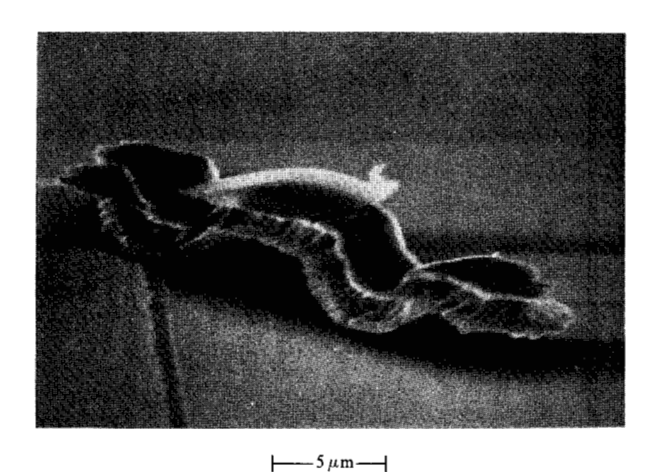


Figure 5 SEM photograph of contact bar made with the double photoresist process. The bar was purposely broken from a switch and is lying upside down.

plated metal bar attached to the end of the membrane is made to connect two metallizations on the surface. Since all the output lines can now be thicker metallizations, much higher currents can be switched.

Initial experiments with the double-contact design exhibited the problem illustrated in Fig. 4(a). Since the photoresist layer over which the Au contacting bar is plated has a sloped edge (for good step coverage during deposition of the plating base), the resulting gradual slope of the plated bar could prevent proper electrical contact if small alignment errors occurred during the etching of the fixed electrodes in a previous step. This problem was solved either by initially plating the fixed electrode regions, as shown in Fig. 4(b), or by applying an additional photoresist layer to construct the more complicated contacting bar shown in Fig. 4(c). Both schemes result in reliable electrical contacts. A SEM photograph of one of these contact bars is shown in Fig. 5. The bar was purposely broken off a switch and is lying upside down on the substrate.

The operating behavior of a micromechanical switch driving a resistive load is shown in Fig. 6. Electrical contact is made about 40  $\mu$ s after the deflection voltage is applied. For somewhat higher deflection voltages, as shown in Fig. 6(b), the contacting electrode strikes the fixed electrode with a higher force and contact bounce is observed. This effect is not unexpected, of course, since these switches are simply very small mechanical relays, i.e., electrostatic versions of the familiar electromagnetic relays in which contact bounce is a well-known phenomenon.

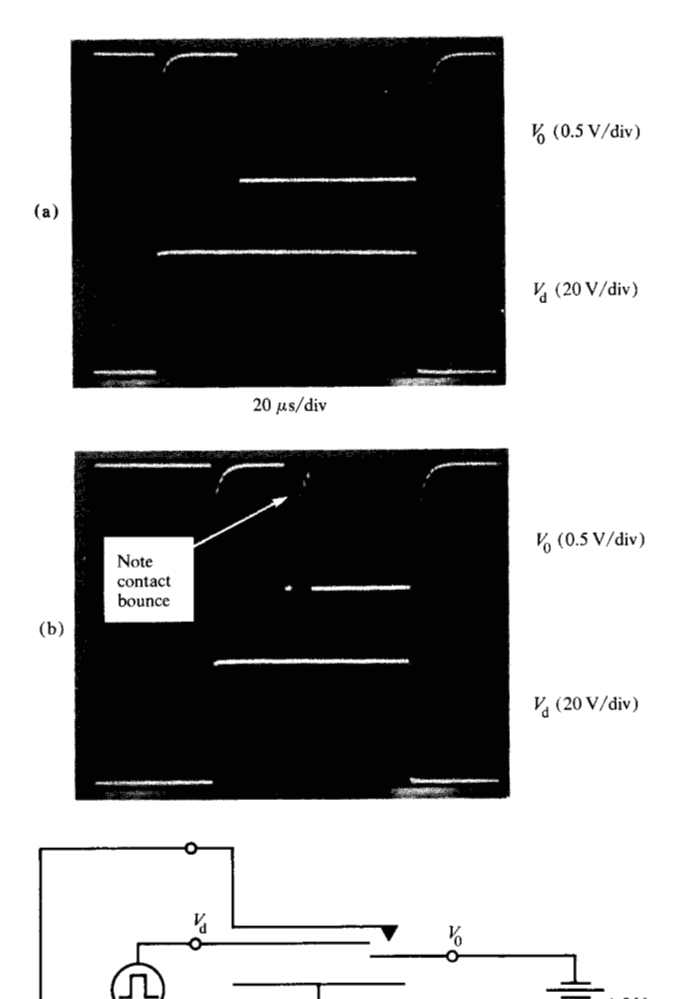
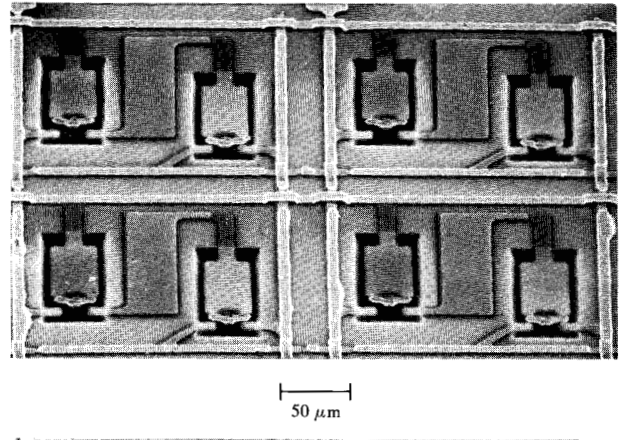


Figure 6 (a) and (b) are oscilloscope traces of typical pulsed switching behavior for the circuit shown in (c). The deflection voltage in (a) is just above the switching threshold (~60 volts), while the voltage in (b) has been increased to about 62 volts. Although the switching delay time is decreased at higher deflection voltages, the probability of contact bounce is increased.

(c)

10 kΩ

Two other well-known and undesirable phenomena of mechanical switches are mechanical fatigue and contact wear. Since work on these micromechanical switches is still in a relatively early stage, no extensive studies of these problems have been completed. Nevertheless, initial results are very encouraging. One of the more important advantages of SiO<sub>2</sub> membranes first pointed out by Thomas *et al.* [17], and one of the motivations for this work, is that under continued flexing, these amorphous elements are less likely to result in fatigue or breakage than metal membranes, which have been employed as deflectable devices in previous studies [18–22]. This as-



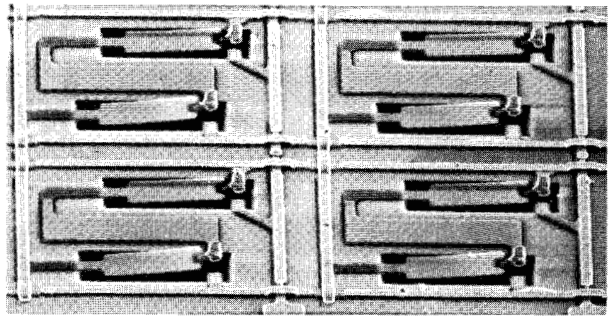


Figure 7 Two views of section of matrix-addressable,  $5 \times 5$  cross-point switching array using two micromechanical switches and a capacitor at each node.

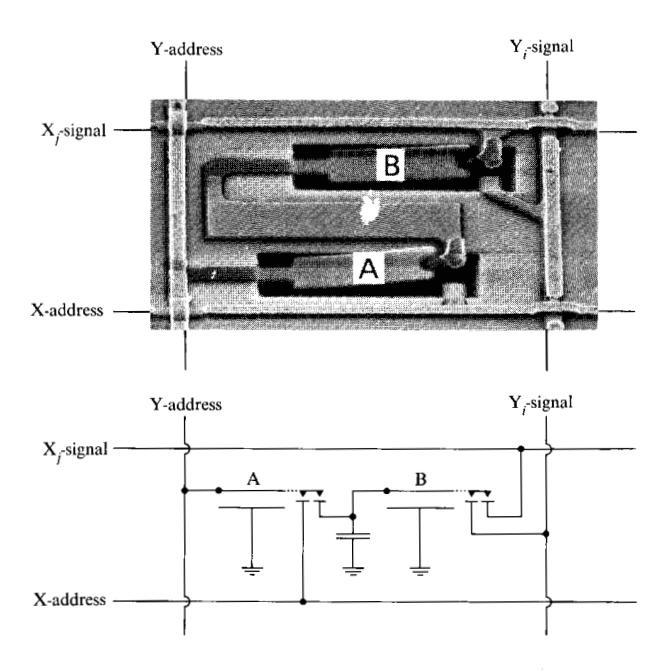


Figure 8 Circuit configuration of each node in the cross-point switch array. Both X-Y address lines and X-Y signal lines pass through each cell. Crossovers are provided by bridges similar to that shown in Fig. 1(a).

sumption was strongly confirmed during a preliminary life test in which simple, metallized SiO<sub>2</sub> membranes (not switches) were flexed, through about 4°, over 10<sup>10</sup> times with no noticeable change in their operational parameters. Membrane breakage has never been observed under ordinary operating conditions.

Contact wear is a different problem which depends critically on the load being driven. Single-contact designs driving resistive loads at current densities over  $5 \times 10^4$  A/cm² (below the level of large electromigration effects) were successfully operated in normal laboratory air over two million times before contact wear effects caused the switch to fail by degradation of the contact resistance. Improved lifetime and reliability are expected in the two-contact design with thick Au conductors and when hermetically sealed in packages with a controlled inert atmosphere. It should be emphasized that these membrane devices are actually quite rugged and can withstand accelerations of hundreds of g's without malfunctioning.

# **Applications**

The unique advantages of micromechanical switches suggest several applications which are difficult or impossible to implement solely with existing, conventional silicon electronic circuitry. One obvious area of potential utility is ac signal switching. All-metal conduction paths, relatively low-resistance metal-to-metal contacts, high or low voltage capability, extremely high off-state resistive impedance, negligible off-state contact coupling capacitance, and low energy switching requirements are the relevant features of micromechanical switches which are particularly important for ac signal switching devices and circuits. Two views from part of a prototype circuit designed to demonstrate this application are illustrated in Fig. 7. The chip is a  $5 \times 5$ , matrix-addressable cross-point switching array. As illustrated in Fig. 8, each node consists of two micromechanical switches and a capacitor. When switch A is addressed by the Y-address line, switch B can be activated with the X-address line, connecting the X<sub>i</sub>-signal input channel to the Y<sub>i</sub>-signal output channel. Switch A can now be deactivated and switch B will remain turned on as long as the capacitor remains charged to the proper voltage level. Switch B is deactivated by addressing switch A on the Y-address line and grounding the X-address line. The circuit is a matrix-addressed cross-point switch array with internal memory. A charge retention time of at least two hours has been demonstrated in a normal laboratory environment. Each switch has the two-contact configuration as shown in Fig. 3(c); the membranes are 0.41  $\mu$ m thick and 83  $\mu$ m in length (70-\mu m-long deflection electrode), suspended over a 6-µm-deep pit. The switches exhibit a contact resistance of less than five ohms, a switching voltage of ~70 volts,

and  $\sim 10~\mu s$  delay time. This contact resistance is higher than that of conventional relays by at least an order of magnitude; however, improvements in design, plating, and cleaning procedures are expected to improve this value. The switching voltage is close to the range normally encountered in conventional telecommunications systems, 48 volts, and can easily be lowered to this level. The switching speed of these devices is at least an order of magnitude faster than that of conventional reed relay switches.

The charge retention capability has other potential applications. In the circuit shown in Fig. 9, for example, the contacting electrode of a micromechanical switch is connected to a variable dc voltage source, while the fixed electrode is connected to a cloverleaf-shaped, deflectable imaging element similar in shape to the mirror matrix light valve elements of Thomas et al. [17]. The four metalcoated SiO<sub>a</sub> leaves are attached to the surface by one corner only and can also be electrostatically deflected toward the bottom of the well when a voltage is applied. Viewed in a microscope under dark-field illumination, the normally undeflected "leaves" appear dark (this is the discharged condition). If the contacting electrode is raised to 16 volts, however, and the switch is activated by a 60-volt pulse, the capacitance between the leaves and the substrate will charge to 16 volts and the leaves will deflect. When the switch is released (after a 100-µs pulse), the leaves will remain charged and, therefore, be stored in the deflected position for at least several hours with no externally applied voltages. When viewed in a microscope under dark-field illumination, the deflected "leaves" appear bright, as shown in Fig. 9(c). Similarly, if the contacting electrode is grounded and the switch is again activated with another 100-µs pulse, the leaves will discharge and return to their undeflected positions.

A large, integrated, matrix-addressable array of similar unit cells, as shown in Figs. 10 and 11, is currently being evaluated. The micromechanical switches are a double-contact design, as shown in Figs. 3(b) and 4(c). The optical element is a single corner-supported deflectable flap; 1260 image storage cells are arranged in a 36-character  $5 \times 7$  format, with three lines of 12 characters each. In addition, 60 peripheral micromechanical switches are used to help decode the incoming data and to reduce the number of chip leads. The chip is a matrix-addressed image storage display, designed to be operated in a simple projection mode.

One potential problem associated with this class of micromechanical devices, which can also be used to advantage, is the bimetallic nature of the membranes. Since SiO<sub>2</sub> and Au exhibit very different thermal coefficients of

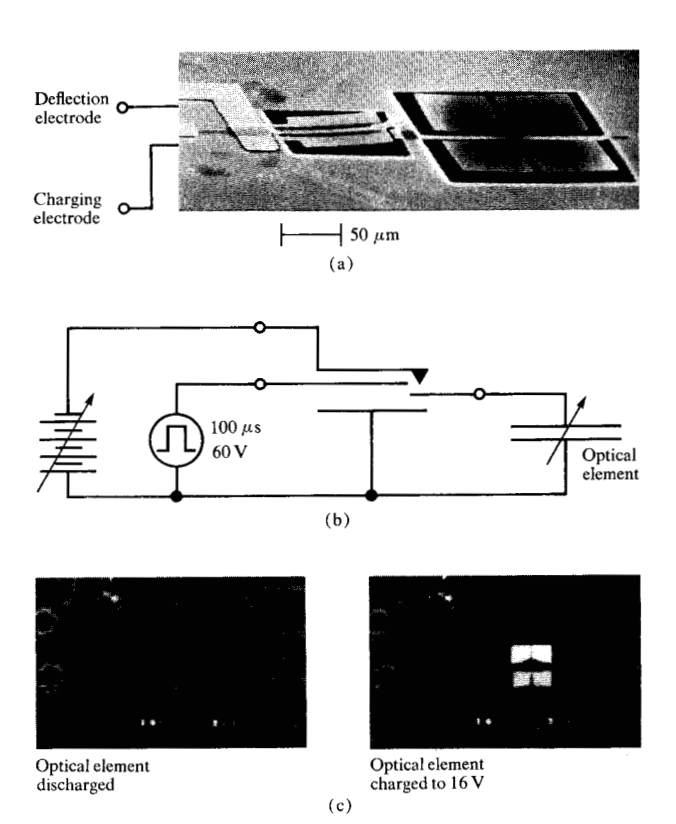
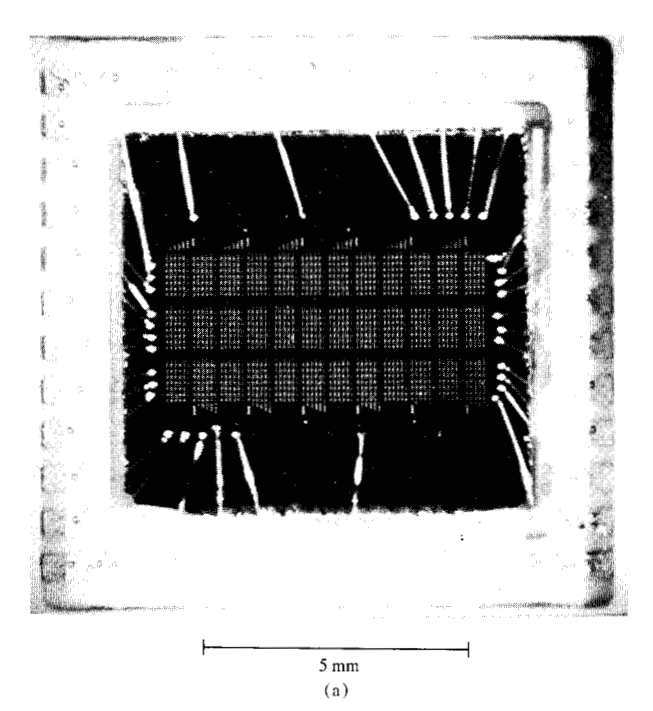


Figure 9 Another charge storage application of micromechanical switches is illustrated by the circuit of (a) and (b). The capacitor leaves can be charged (and, therefore, deflected) by increasing the charging voltage to 16 volts and pulsing the switch for  $100~\mu s$ . They will remain stored in this deflected position, shown at the right in (c), until the switch is pulsed again with the charging voltage reduced to zero, thereby releasing the leaves back to their discharged, or undeflected, positions.

expansion, increases in temperature result in a downward deflection of the membrane. Normally-open switches will then close at a given temperature, depending on the switch geometry, film thicknesses, and initial membrane deflection, if any. In particular, in an array of simple switches, all with slightly different lengths, each switch will make electrical contact at a different temperature. As the membrane length  $(\ell)$  decreases, the contacting temperature increases, since the deflection of the membrane tip (D) can be expressed by

$$D = \frac{\ell^2}{t} K \Delta \alpha \Delta T, \tag{1}$$

where t is the total membrane thickness,  $\Delta \alpha$  is the difference in thermal coefficients of expansion of the metal and the SiO<sub>2</sub>, K is a constant which depends on the ratio of the thicknesses of the two layers and the ratio of Young's modulus of the two layers, and  $\Delta T$  is the temperature rise above ambient.



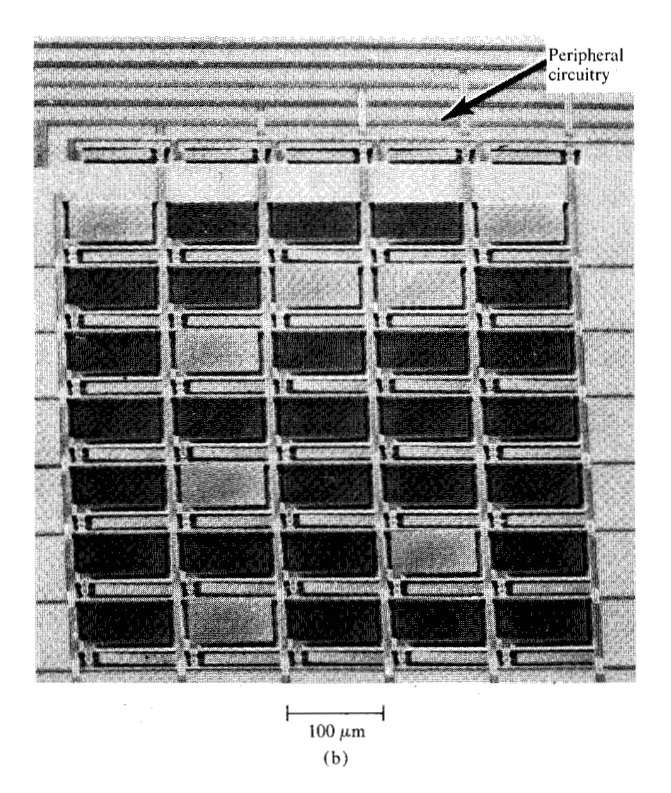


Figure 10 (a) Overall optical photograph of experimental 1260-cell, 36-character optical storage and display chip. (b) Closer view of a single  $5 \times 7$  character array, showing a portion of the peripheral circuitry used to help decode the matrix-addressed data. Each cell contains a micromechanical switch like that in Fig. 1(b) and a single corner-supported deflectable flap.

To demonstrate this threshold temperature sensing concept, the circuit of Fig. 12 was evaluated. The threshold temperature of a single switch can be decreased by applying a bias voltage. The data shown in Fig. 13 were taken by keeping the bias voltage constant and increasing the temperature until the switch closed. A small hysteresis will be observed as the temperature is lowered back below this threshold point.

## **Future developments**

In addition to more extensive characterization and analysis of the performance and reliability of these switches to determine and evaluate areas of applicability, two lines of research are being pursued to develop new devices and new effects using membranes.

Since the individual switches and circuits described here do not make use of the electronic properties of single-crystal silicon, procedures can be formulated to fabricate these devices from deposited films on other substrates. The fully operational switch shown in Fig. 14, for example, was fabricated from sputtered films of Cr (substituting for the buried p<sup>+</sup> stopping layer and bottom deflection electrode),  $\alpha$ -Si (replacing the epitaxial spacing layer), and SiO<sub>a</sub> (instead of a thermally grown film). Of course, without a single-crystal epitaxial layer, lateral undercutting cannot be controlled with the anisotropic etchant. As a result, the oxide around the periphery of individual switches will necessarily be significantly undercut and somewhat warped, as shown by the wide, lighter region surrounding the switch in Fig. 14. A solution to this problem would be to etch "mesas" from the sputtered silicon (before depositing the membrane oxide) wherever a switch is desired to control undercutting and alleviate warping. Not only does this fabrication procedure permit the use of other substrates, but all the processing steps are at low temperature, thus allowing greater versatility in choice of materials, design, and applications.

At the other extreme, interesting and exotic effects and circuits might be obtained by combining micromechanical switches on the same chip with conventional silicon integrated circuitry. Some of these possibilities are now being investigated. The rapidly decreasing costs of integrated circuit chips, together with the high costs and increasing importance of sensors and actuators in microprocessor control systems, may combine to make this integration economically viable.

#### Discussion

A new class of devices involving electrostatically deflectable oxide membranes has been developed. Although these devices are fabricated on silicon using processes compatible with conventional integrated circuit techniques, their unique characteristics have made it possible to demonstrate applications difficult or impossible to realize with conventional silicon devices.

The fundamentals of the technology are so new, however, that extensive evaluations of lifetime and reliability have yet to be completed. Nevertheless, the fabrication principles are not only based on highly reliable materials (e.g.), amorphous  $\mathrm{SiO}_2$  instead of plated metal for the deflectable member; gold for the contacting points), but are also highly adaptable and designable to new applications or situations, or to resolve operational problems as discussed above. In addition, results of preliminary lifetime studies appear promising.

The ultimate areas of applicability of these switches will surely depend on the ultimate performance parameters attainable. It is clear, for example, that a trade-off exists between high frequency and current-carrying capability. The resonant frequency of a simple cantilever beam, of length  $\ell$  and thickness t with a mass M (the contacting bar) attached to the tip, is given by [26]

$$f_{\rm R} = \frac{1}{2\pi} \sqrt{\frac{3EI}{\ell^3 (M + 0.23m)}} \quad , \tag{2}$$

where E is Young's modulus for  $SiO_2$ , I is the moment of inertia of the beam, and m is its mass. For high currents, the mass of the contacting bar M must be large, thereby mechanically loading the membrane tip and reducing the maximum operating frequency. On the other hand, a trade-off also exists between switching voltage and resonant frequency. A characteristic threshold voltage may be defined for electrostatically deflectable cantilever beams of the type described here [16]:

$$V_{\rm th} \simeq \sqrt{\frac{18EId^3}{5\varepsilon_0 \ell^4 b}} \quad , \tag{3}$$

where d is the depth of the well under the beams, b is the width of the beam, and  $\varepsilon_0$  is the permittivity of free space. Comparing Eqs. (2) and (3), we see that changes in the membrane geometry affect both parameters in a similar manner, so that low deflection voltage geometries also imply low resonant frequencies or long delay times between the application of the deflection voltage pulse and the switch closure.

From these considerations it is clear that optimization of resonant frequency (or delay time), deflection voltage, and current-carrying capability must be performed case by case, depending on the desired function of the device or circuit. Nevertheless, it is also obvious that these are not *very* high speed nor *very* low voltage devices com-

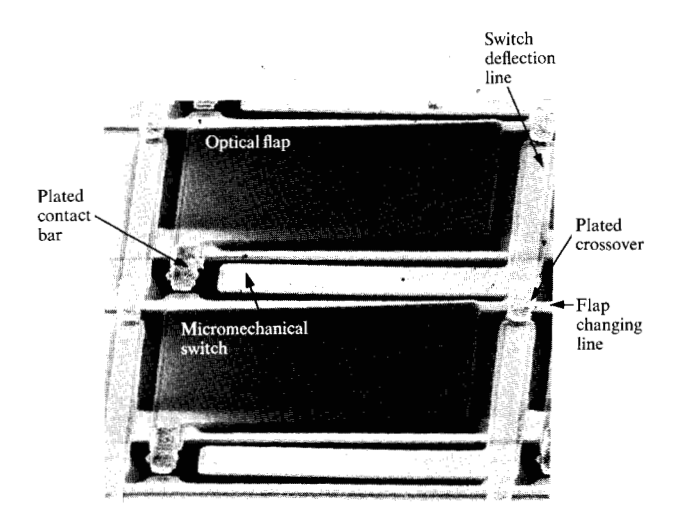
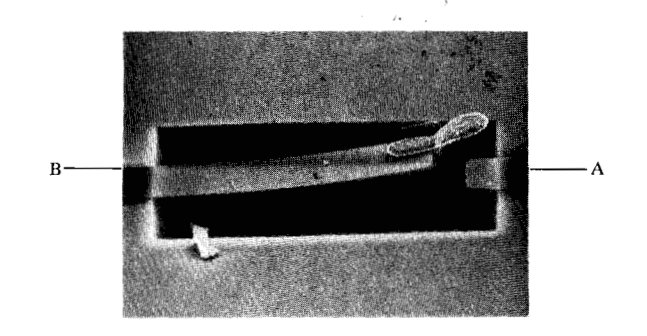
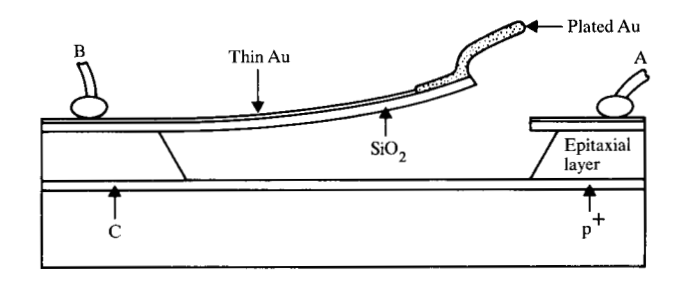


Figure 11 Two complete image storage cells from Fig. 10, showing double-contact switch, deflectable flap, plated metal crossover, and double-photoresist contact bar.





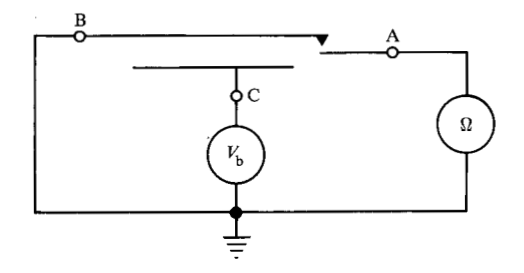


Figure 12 Three-terminal micromechanical switch used in a temperature sensing demonstration, based on the differences in thermal coefficients of expansion between  $\mathrm{SiO_2}$  and the Cr-Au metallization. Variation of the bias voltage  $V_\mathrm{b}$  will change the temperature at which the switch closes.

383

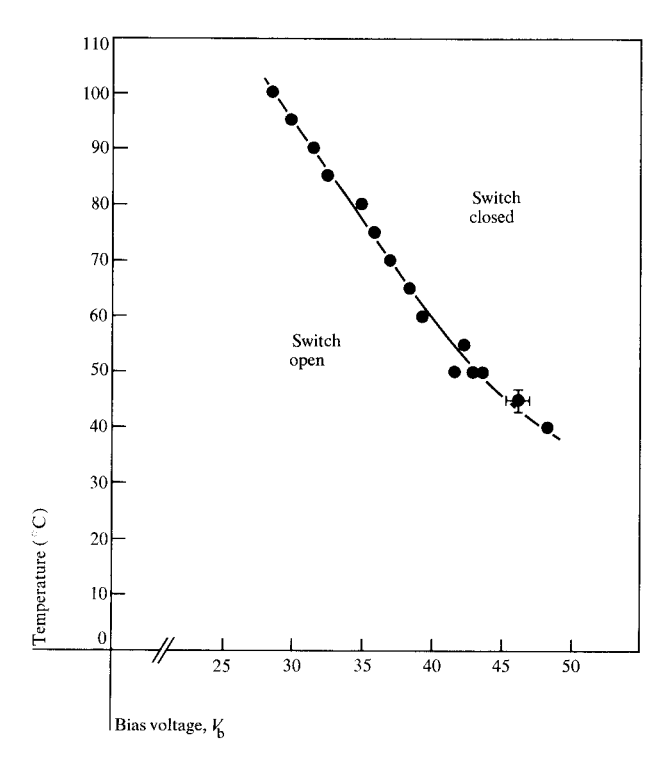
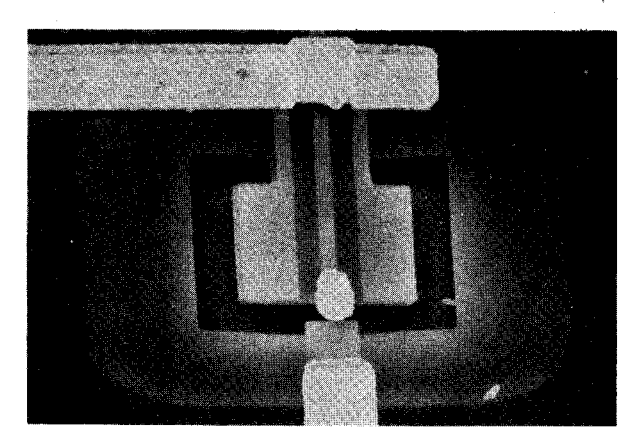


Figure 13 Threshold switching temperature of the device shown in Fig. 12 as a function of bias voltage.



**⊢**20 μm**⊣** 

Figure 14 SEM photograph of a fully operational micromechanical switch fabricated entirely from sputtered layers. Note the undesirable lateral undercutting around the switch periphery (the lightly shaded region) and the potentially troublesome warping of the thin oxide (reasons described in the text).

pared to transistors, nor are they very high current switches compared to electromagnetic relays. Micromechanical switches thus appear to be capable of filling the gap between these two well-established technologies. With 3- to 4- $\mu$ m design rules, frequency and voltage can probably be optimized in the 200-kHz, 20- to 30-volt range for low currents, while even high-current devices of the type described here will likely be limited to less than one ampere.

Contact resistance is another parameter which must be improved. As mentioned previously, the value of five ohms observed thus far is expected to decrease substantially through optimization of the design, as well as the plating and cleaning procedures.

As already discussed, these switches are ideally suited in signal switching applications or in any circuit where extremely high off-on impedance ratios are important. Since they are batch fabricated using silicon integrated circuit technology, they can also be easily processed, inexpensively, in large integrated arrays. Finally, their compatibility with conventional silicon circuitry suggests that further novel extensions of this technology may be expected.

The micromechanical switch herein described is only one in a series of new devices in a rapidly expanding extension of silicon technology. It is becoming more and more likely that silicon will be increasingly called upon, not only in an electronic role, but also in a wide range of mechanical capacities where small, high-accuracy, high-reliability, and low-cost mechanical components and/or devices are required in critical applications, performing functions not ordinarily associated with silicon.

# **Acknowledgments**

The author thanks L. Holland, A. Shartel, L. Smith, W. Ko, F. Anger, R. Tom, and J. Hope for technical assistance; V. Hanchett for the photographs; and R. V. Pole, G. T. Sincerbox, and N. Platakis for stimulating discussions.

#### References

- 1. M. P. Lepselter, "Silicon Technology: The New Steel," *International Electron Devices Meeting Proceedings*, Washington, D.C., 1974, p. 9.
- E. Bassous, H. H. Taub, and L. Kuhn, "Ink Jet Printing Nozzle Arrays Etched in Silicon," Appl. Phys. Lett. 31, 135 (1977).
- 3. E. Bassous, "Fabrication of Novel Three-Dimensional Microstructures by the Anisotropic Etching of (100) and (110) Silicon," *IEEE Trans. Electron Devices* ED-25, 1178 (1978).
- L. Kuhn, "Recording Apparatus Having a Semiconductor Charge Electrode," U.S. Patent 3,984,843, 1978.
- S. C. Terry, "A Gas Chromatography System Fabricated on a Silicon Wafer Using Integrated Circuit Technology," Ph.D. Thesis, Stanford University, Stanford, CA, 1975.
- L. Roylance and J. B. Angell, "A Miniature Silicon Accelerometer for Biomedical Applications," *International Solid State Circuits Conference Proceedings*, San Francisco, February 1978.

K. E. PETERSEN

- W. T. Tsang, C. C. Tseng, and S. Wang, "Optical Wave-guides Fabricated by Preferential Etching," Appl. Opt. 14, 1200 (1975).
- 8. Chenming Hu and Seihee Kim, "Thin-Film Dye Laser with Etched Cavity," Appl. Phys. Lett. 29, 9 (1976).
- J. T. Boyd and S. Sriram, "Optical Coupling from Fibers to Channel Waveguides Formed on Silicon," Appl. Opt. 17, 895 (1978).
- J. S. Harper and P. F. Heidrich, "High Density Multichannel Optical Waveguides with Integrated Couplers," Wave Electron. 2, 369 (1976).
- 11. H. P. Hsu and A. F. Milton, "Single Mode Optical Fiber Pick-Off Coupler," Appl. Opt. 15, 2310 (1976).
- 12. H. P. Hsu and A. F. Milton, "Single-Mode Coupling between Fibers and Indiffused Waveguides," *IEEE J. Quantum Electron.* **QE-13**, 224 (1977).
- J. D. Crow, L. D. Comerford, R. A. Laff, M. J. Brady, and J. S. Harper, "GaAs Laser Array Source Package," Opt. Lett. 1, 40 (1977).
- 14. W. A. Little, "Design and Construction of Microminiature Cryogenic Refrigerators," presented at the conference on "Future Trends in Superconductive Electronics," University of Virginia, Charlottesville, VA, March 1978.
- 15. K. E. Petersen, "Micromechanical Light Modulator Array Fabricated on Silicon," Appl. Phys. Lett. 31, 521 (1977).
- K. E. Petersen, "Dynamic Micromechanics on Silicon: Techniques and Devices," *IEEE Trans. Electron Devices* ED-25, 1241 (1978).
- R. N. Thomas, J. Guldberg, H. C. Nathanson, and P. R. Malmberg, "The Mirror Matrix Tube: A Novel Light Valve for Projection Displays," *IEEE Trans. Electron Devices* ED-22, 765 (1975).
- 18. J. A. van Raalte, "A New Schlieren Light Valve for Television Projection," Appl. Opt. 9, 2225 (1970).

- 19. Kendall Preston, Jr., "A Coherent Optical Computer System Using the Membrane Light Modulator," *IEEE Trans. Aerospace Electr. Syst.* **AES-6**, 458 (1970).
- L. S. Cosentino and W. C. Stewart, "A Membrane Page Composer," RCA Rev. 34, 45 (1973).
- W. D. Frobenius, S. A. Zeitman, M. H. White, D. D. O'Sullivan, and R. G. Hamel, "Microminiature Ganged Threshold Accelerometers Compatible with Integrated Circuit Technology," *IEEE Trans. Electron Devices* ED-19, 37 (1972).
- 22. H. C. Nathanson, W. E. Newell, R. A. Wickstrom, and J. R. Davis, Jr., "The Resonant Gate Transistor," *IEEE Trans. Electron Devices* ED-14, 117 (1967).
- 23. R. M. Finne and D. L. Klein, "A Water-Amine-Complexing Agent System for Etching Silicon," J. Electrochem. Soc. 114, 965 (1967).
- 24. A. Bohg, "Ethylene-Diamine-Pyrocatechol-Water Mixture Shows Etching Anomaly in Boron-Doped Silicon," *J. Electrochem. Soc.* **118**, 401 (1971).
- I. J. Pugacz-Muraszkiewicz, "Detection of Discontinuities in Passivating Layers on Silicon by NaOH Anisotropic Etch," IBM J. Res. Develop. 16, 523 (1972).
- 26. J. P. Den Hartog, *Mechanical Vibrations*, McGraw-Hill Book Co., Inc., New York, 1956, p. 432.

Received November 31, 1978; revised February 22, 1979

The author is located at the IBM Research Division laboratory, 5600 Cottle Road, San Jose, California 95193.